RESEARCH ARTICLE

WILEY

Orientational changes of white matter fibers in Alzheimer's disease and amnestic mild cognitive impairment

Haichao Zhao[1] | Jian Cheng[2] | Tao Liu[1,2] (iD) | Jiyang Jiang[3] | Forrest Koch[3] | Perminder S. Sachdev[3] (iD) | Peter J. Basser[4] | Wei Wen[3] | for the Alzheimer's Disease Neuroimaging Initiative

[1]Beijing Advanced Innovation Center for Biomedical Engineering, School of Biological Science and Medical Engineering, Beihang University, Beijing, China

[2]Beijing Advanced Innovation Center for Big Data-Based Precision Medicine, Beihang University, Beijing, China

[3]Centre for Healthy Brain Ageing, School of Psychiatry (CHeBA), University of New South Wales, Sydney, New South Wales, Australia

[4]Section on Quantitative Imaging and Tissue Sciences, NIBIB, NICHD, National Institutes of Health, Bethesda, Maryland

Correspondence
Tao Liu, School of Biological Science and Medical Engineering, International Research Institute for Multidisciplinary Science, IRC 300, Beihang University, Beijing 100191, China.
Email: tao.liu@buaa.edu.cn

Abstract

White matter abnormalities represent early neuropathological events in neurodegenerative diseases such as Alzheimer's disease (AD), investigating these white matter alterations would likely provide valuable insights into pathological changes over the course of AD. Using a novel mathematical framework called "Director Field Analysis" (DFA), we investigated the geometric microstructural properties (i.e., splay, bend, twist, and total distortion) in the orientation of white matter fibers in AD, amnestic mild cognitive impairment (aMCI), and cognitively normal (CN) individuals from the Alzheimer's Disease Neuroimaging Initiative 2 database. Results revealed that AD patients had extensive orientational changes in the bilateral anterior thalamic radiation, corticospinal tract, inferior and superior longitudinal fasciculus, inferior fronto-occipital fasciculus, and uncinate fasciculus in comparison with CN. We postulate that these orientational changes of white matter fibers may be partially caused by the expansion of lateral ventricle, white matter atrophy, and gray matter atrophy in AD. In contrast, aMCI individuals showed subtle orientational changes in the left inferior longitudinal fasciculus and right uncinate fasciculus, which showed a significant association with the cognitive performance, suggesting that these regions may be preferential vulnerable to breakdown by neurodegenerative brain disorders, thereby resulting in the patients' cognitive impairment. To our knowledge, this article is the first to examine geometric microstructural changes in the orientation of white matter fibers in AD and aMCI. Our findings demonstrate that the orientational information of white matter fibers could provide novel insight into the underlying biological and pathological changes in AD and aMCI.

KEYWORDS
Alzheimer's disease, amnestic mild cognitive impairment, geometric microstructure, orientation change, white matter

Haichao Zhao and Jian Cheng are joint first authors.

Data used in preparation of this article were obtained from the Alzheimer's Disease Neuroimaging Initiative (ADNI) database (adni.loni.usc.edu). As such, the investigators within the ADNI contributed to the design and implementation of ADNI and/or provided data but did not participate in analysis or writing of this report. A complete listing of ADNI investigators can be found at: http://adni.loni.usc.edu/wp-content/uploads/how_to_apply/ADNI_Acknowledgement_List.pdf.

1 | INTRODUCTION

Alzheimer's disease (AD) is a neurological disorder characterized by amyloid-β plaques and neurofibrillary tangles in the gray matter, with associated inflammation and neuronal death (Braak & Braak, 1991; Braak & Braak, 1995). In addition to prominent gray matter atrophy, there is myelin degeneration and axonal loss in neural fiber tracts (Bartzokis, 2011; Hua et al., 2013), leading to significant white matter damage (Apostolova et al., 2010; Apostolova & Thompson, 2008; Chintamaneni & Bhaskar, 2012; Desikan, et al., 2010; Leung et al., 2013). The neurodegeneration in AD is known to begin 20–30 years before clinical symptoms (e.g., amnestic mild cognitive impairment, aMCI) become apparent (Chintamaneni & Bhaskar, 2012). Treatments are most likely to be effective before pathological changes spread throughout the brain. Thus, an early diagnosis with reliable biomarkers is essential for the development of effective treatment and/or prevention strategies.

Although many researchers have examined AD from the perspective of functional network-based dysfunctions (Canter, Penney, & Tsai, 2016; Palop, Chin, & Mucke, 2006), direct investigation of white matter abnormalities may provide novel insights into the pathophysiology of AD (Langen et al., 2017; Mito et al., 2018). Diffusion tensor imaging (DTI) is a powerful and noninvasive neuroimaging technique for in vivo mapping of white matter changes in the human brain. DTI provides voxel-based metrics, such as fractional anisotropy (FA) and mean diffusivity (MD). Among the tensor-derived metrics, FA is one of the most popular and effective measures (Taylor, Hsu, Krishnan, & MacFall, 2004). It describes the anisotropy of water diffusion, which is reflective of the degree of directionality of cellular structures within a voxel. One major limitation of those classical metrics is the difficulty to model voxels containing multiple fiber populations (Jones, Knösche, & Turner, 2013; O'Donnell & Pasternak, 2015). Despite this, the loss of anisotropic diffusion tends be to some extent related to the demyelination of white matter fibers and axonal loss (Jones et al., 2013; Leung et al., 2004). Numerous DTI-based AD studies have reported reductions in white matter microstructural integrity as indicated by voxel-based metrics (e.g., FA and MD; Gold, Johnson, Powell, & Smith, 2012; Minati, Edginton, Grazia Bruzzone, & Giaccone, 2009; Nachev, Wydell, O'neill, Husain, & Kennard, 2007; Nir et al., 2013; Taylor et al., 2004).

Aside from this, another limitation of classical tensor framework is its inability to demonstrate the directional diffusion based on the voxel analysis. The traditional DTI framework utilizes intra-voxel information to describe the spatial diffusion within a single voxel, to some extent reflect on the integrity of microstructure of white matter fibers. It does not utilize inter-voxel information to represent for the orientational properties of microstructure in the white matter fibers in a spatial neighborhood. Numerous morphological studies have revealed that AD and aMCI had gross white matter atrophy and gray matter loss (Balthazar et al., 2009; Ferreira, Diniz, Forlenza, Busatto, & Zanetti, 2011; Guo et al., 2010; Tabatabaei-Jafari, Shaw, & Cherbuin, 2015). Ventricular dilation has also been found to correlate with aging-related pathologies, such as aMCI and AD (Biegon

et al., 1994; Bramlett & Dietrich, 2002; Chou et al., 2009; Thompson et al., 2004). Thus, these morphological changes may compress or pull the local white matter fiber, thereby distorting the orientational distribution in the local white matter. In addition, histological and ultrastructural evidences from the Alzheimer's mouse model, as well as post-mortem examination of humans, have indicated that AD can lead to neuron numbers reduction, glial swelling, and demyelination in local white matter regions (Qin et al., 2013; Shu et al., 2013; Zerbi et al., 2013). Given the role of glial cells in the physical support for neurons, swollen glia cells and loss of neuron itself may cause the orientational distortion of local white matter fibers. In brief, the morphological and histological alteration in AD could be potential factors inducing the orientational changes in the white matter fibers. Intravoxel diffusion information alone, obtained by the methods mentioned above, would not be able to describe such orientational changes of white matter fibers. Therefore, it is urgent to apply a novel method for complementing the deficiency of classical metrics on such geometric microstructural changes in the orientation of white matter fiber in AD and aMCI.

Recently, a novel mathematical framework called Director Field Analysis (DFA), inspired by the microscopic theoretical treatment of phases in liquid crystals, was proposed to study the orientational distortion of local white matter based on the reconstructed tensor field or spherical function field (Cheng & Basser, 2017). In the studies of liquid crystals, change in the orientations of rod-like molecules is called as "orientational distortion." Compared to conventional intra-voxel-based metrics that only provide intra-voxel information (e.g., FA and MD), DFA provides inter-voxel information which allows for measuring the orientational changes of local white matter fibers. Specifically, DFA provides three orientational indices: splay, bend, and twist, as shown in Figure 1, and a total distortion index to quantify the orientational properties in a local spatial neighborhood. We hypothesized that DFA may supplement the deficiency of classical DTI metrics in exploring the orientational changes of white matter fiber tracts, which may in turn suggest the new pathological evidences in AD and aMCI that have not been explored.

In this study, we present the first application of the geometric microstructural information in the orientation of local white matter fibers in individuals with AD ($n = 48$) and aMCI ($n = 56$) in comparison to CN ($n = 60$). The purpose of this study was to evaluate the specific pattern of orientational changes of local white matter fibers in AD and aMCI, and to investigate the possible cause of the local white matter orientational changes in AD and aMCI.

2 | MATERIALS AND METHODS

All data used in this study were obtained from the Alzheimer's Disease Neuroimaging Initiative 2 (ADNI2; http://adni.loni.usc.edu). The ADNI was launched in 2003 as a public–private partnership, led by Principal Investigator Michael W. Weiner, MD. The primary goal of ADNI has been to test whether serial MRI, positron emission tomography (PET), other biological markers, and clinical and neuropsychological
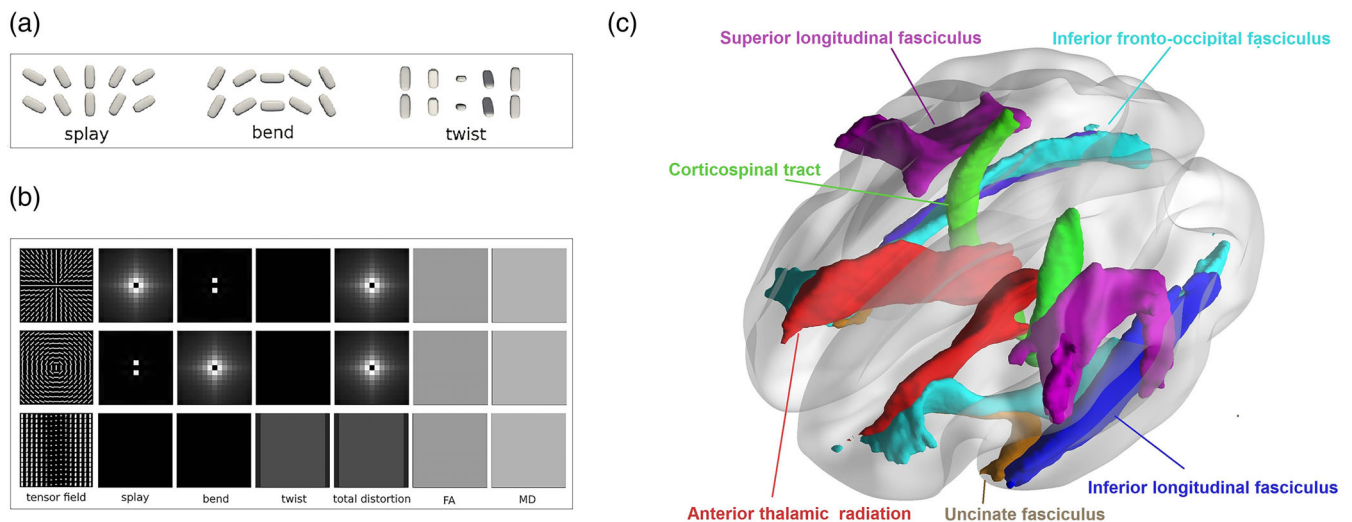
FIGURE 1 (a) A brief illustration of three types of orientational distortions (i.e., splay, bend, and twist). The figure was revised and approved from Cheng and Basser (2017). (b) Each row shows a synthetic tensor field with the six index maps (splay, bend, twist, total distortion, FA, and MD) calculated from the tensor field. All tensors in the tensor fields share the same shape but have different orientations, resulting in constant FA and MD maps. While the new orientational indices (splay, bend, twist and total distortion) could reflect the local spatial orientational distortions. (c) Tracts of interest, including anterior thalamic radiation, uncinate fasciculus, inferior longitudinal fasciculus, inferior fronto-occipital fasciculus, superior longitudinal fasciculus and corticospinal tract. FA, fractional anisotropy; MD, mean diffusivity

assessment could be combined to measure the progression of aMCI and early AD. Determination of sensitive and specific markers of very early AD progression was intended to aid researchers and clinicians to develop new treatments and monitor their effectiveness, as well as lessen the time and cost of clinical trials.

2.1 | Participants

This study included individuals with AD, aMCI, and CN, from ADNI2. The inclusion criterion was: (a) each subject must have completed both T1-weighted images and DWI images; (b) AD patients met the National Institute of Neurological and Communicative Disorders and Stroke and the Alzheimer's Disease and Related Disorders Association (NINCDS/ADRDA) criteria for probable AD, had a Mini-Mental State Exam (MMSE) score below 26, had a Clinical Dementia Rating above 0.5, and had an abnormal memory function documented by the Wechsler Memory Scale—Revised; (c) aMCI individuals were classified by a clinical review panel, with a score between 24 and 30 on MMSE, a Clinical Dementia Rating of 0 or 0.5, and an abnormal memory function; (d) CN individuals were required to be free of subjective memory concerns, had a MMSE score between 24 and 30, and a Clinical Dementia Rating of 0.

Our study, therefore, initially had 50 AD patients, 56 aMCI patients, and 60 CN individuals from ADNI2. Among the AD patients, two were removed because of the incomplete DTI data. The final cohort included 48 AD patients (18 F/30 M, 76.33 ± 8.58 years old, MMSE = 21 ± 4.5), 56 aMCI patients (23 F/33 M, 73.39 ± 8.18 years old, MMSE = 27.75 ± 1.7), and 60 CN individuals (32 F/28 M, 76.2 ± 6.65 years old, MMSE = 28.62 ± 1.82). The characteristics of all

participants are shown in Table 1. All participants had given their informed written consent approved by each sites' Institutional Review Board.

2.2 | Image acquisition

All participants underwent whole-brain MRI scans using the ADNI protocol. All MRI were carried out using 3 T MRI scanners (GE Medical Systems) from seven North American sites. Sagittal MPRAGE T1-weighted scans were acquired with the following parameters: TR = 7.34 ms; TE = 3 ms; TI = 400 ms; FA =11°; acquisition matrix = 256 × 256; number of slices = 180, yielding scans with voxel size = 1 × 1 × 1.2 mm^3. Axial diffusion weighted image data were acquired with a spin echo planar imaging sequence with the following parameters: acquisition matrix = 256 × 256, voxel size = 1.4 × 1.4 × 2.7 mm^3; flip angle = 90°; number of slices = 59. There were 46 images acquired for each scan: 41 diffusion-weighted images (b = 1,000 s/mm^2), and 5 non-diffusion-weighted images (b = 0 s/mm^2). Repetition time varied across scanning sites, and was approximately between 12,500 and 13,000 ms.

2.3 | Image pre-processing

Briefly, the ADNI2 DICOM files were converted to NIFTI files with MRIcron's dcm2nii. We then used FSL 5.0.9 (fMRIB Software Library, www.fmrib.ox.ac.uk/fsl) to correct eddy current distortions and head movement. We adjusted the gradient directions based on the eddy current correction. BET was then used to remove non-brain tissue

	CN	MCI	AD	F/χ^2	p
n	60	56	48	#	#
Age, years (SD)	76.2 (6.65)	73.39 (8.18)	76.3 (8.58)	2.459	.089
Males (%)	28 (46.7%)	33 (58.9%)	30 (62.5%)	2.390	.122
CDR (SD)	0.08 (0.2)	0.48 (0.13)	1.06 (0.43)	171.730	<.001
MMSE (SD)	28.62 (1.82)	27.75 (1.7)	21 (4.5)	107.739	<.001

TABLE 1 Clinical and demographic characteristics of each diagnostic group

Note: Data are presented as mean and *SD* or percentage number (%). Reported *p*-values were obtained from one-way between-groups ANOVA tests for age, CDR, and MMSE scores, and chi-square test for independence for sex.
Abbreviations: AD, Alzheimer's disease patients; CDR, clinical dementia rating; HC, healthy elderly control subjects; MCI, mild cognitive impairment; MMSE, Mini-Mental State Examination.

(Smith, 2002), and brain-extracted images were visually inspected. The local PCA algorithm implemented in Dipy (https://dipy.org/) was applied to denoise the acquired diffusion data. In addition, corrected b0 images were linearly aligned to skull-stripped T1 images using FSL linear registration with boundary-based registration. The linearly aligned b0 image was then nonlinearly registered to the T1-weighted images with ANTs (http://stnava.github.io/ANTs/) to correct for EPI-induced susceptibility artifacts. Finally, the resultant 3D deformation fields were then applied to the remaining diffusion data.

We used DMRITool (http://diffusionmritool.github.io) to reconstruct diffusion tensors, and calculate six DTI metric maps, including FA, MD, and four DFA metrics: splay, bend, twist, and total distortion (Cheng & Basser, 2017) for each subject. Detailed interpretations for DFA metrics have been described by Cheng and Basser (2017), which are summarized in brief below.

2.4 | DFA metrics

We used a novel mathematical framework DFA to compute the orientational distortion of local white matter fibers based on tensor images. Based on studies of liquid crystals, there are three types of orientational distortions, that is, splay, bend, and twist. See Figure 1a.

1. Splay: spatial bending occurs perpendicular to the direction of the main molecular axis;
2. Bend: spatial bending is parallel to the direction of the main molecular axis;
3. Twist: neighboring directions are rotated with respect to one another, rather than aligned.

The three tensor fields in Figure 1a demonstrate splay, bend, and twist of the orientational distortions in a local neighborhood. Figure 1b shows three synthetic tensor fields with their six index maps (splay, bend, twist, total distortion, FA, and MD). All tensors in these three tensor fields have the same shape (i.e., the same tensor-derived indices, for example, FA or MD), but spatially different orientations. Intra-voxel tensor-derived index maps (e.g., FA or MD) cannot distinguish these local geometric microstructures formed by inter-voxel orientational changes. Both FA and MD are constant maps

because all tensors have the same shape. DFA provides splay, bend, and twist indices to describe these three local geometric microstructures of orientational distortion, and a total orientational distortion index to describe a combination of all three types. The main idea of DFA is to construct a local orthogonal frame at each voxel, where the first axis is the main direction of that voxel, and then define these inter-voxel DFA indices (splay, bend, twist) using spatial derivatives of the main direction along different axes (Cheng & Basser, 2017). After defining splay, bend, twist indices, the total distortion index is defined as square root of the sum of square of these three indices (total distortion $= \sqrt{splay^2 + bend^2 + twist^2}$). See Cheng and Basser (2017) for more detailed definitions of DFA indices. Using DFA indices, we can quantify the local geometric microstructures in the orientation of white matter fibers in a local neighborhood at an inter-voxel level. See Figure 1. The first row in Figure 1b shows a tensor field with a circular splay pattern, where tensor orientations splay around the central voxel. Ignoring the singularity of the central voxel, both the bend and twist indices are zero, and the splay index quantifies the degree of splay. The second row in Figure 1b shows a tensor field with a circular bend pattern, where tensor orientations bend around the central voxel. Both the splay and twist indices are zero, and the bend index quantifies the degree of bend. The third row in Figure 1b shows a twist pattern, where from left to right in each row a tensor twists its orientation around the left–right axis. The twist index map is constant for this tensor field, ignoring the boundary effect in the calculation of the boundary voxels of the field, while both splay and bend maps are zero. Although in these three tensor fields, only one index map among splay, bend and twist maps is nonzero, these three index maps are normally all non-zero for real data, because the spatial orientational distortion normally happens in the three-dimensional space for real data, not in a two-dimensional space as synthesized in Figure 1.

3 | STATISTICAL ANALYSIS

3.1 | Tract-based spatial statistics (TBSS)

Mean FA maps were created and thinned to obtain a projection of all participants' FA data onto a mean FA skeleton that represented the

centers of all tracts common to the group (Smith et al., 2006). Briefly, all participants' FA data were nonlinearly aligned to a standard template space (FMRIB58_FA). Then, the mean FA image was created and thresholded (FA value >0.2) to create the mean FA skeleton. Next, each participant's FA data was projected onto the thresholded mean FA skeleton. In addition, TBSS was also performed for the four DFA indices (splay, bend, twist, and total distortion). The displacement fields of the non-linear registration estimated from the FA images were applied to warp DFA index maps. The warped maps were subsequently projected onto the mean FA skeleton before applying voxel-wise statistics. Finally, a general linear model built with group factor as independent factors, demeaned age, gender and scanner sites as nuisance covariates. Voxel-wise statistical analysis of white matter skeleton was conducted with permutation-based nonparametric inference on the FA, MD and DFA indices using Randomize to assess group difference between AD and CN, and between aMCI and CN. Threshold Free Cluster Enhancement (TFCE; Smith & Nichols, 2009) was used to correct for multiple comparisons across the whole brain ($p < .05$).

Besides, to visually show the geometric microstructural difference between AD, aMCI and CN, we would select the white matter regions where DFA indices (e.g., bend) but not FA had significant difference, and visualize their tensor fields using DFA indices and FA.

3.2 | Tracts of interest analysis

We performed tracts of interest analysis to investigate potential changes of selective fiber pathways in aMCI participants. The white matter tracts of interest were identified with Johns Hopkins University's white matter atlas available in FSL (Mori et al., 2008; Wakana et al., 2007). Based on the TBSS results of DFA indices, we selected all the regions which showed significant changes in the total distortion in AD patients, and categorized these regions into six tracts of interest—namely, the anterior thalamic radiation, uncinate fasciculus, inferior longitudinal fasciculus, corticospinal tract, superior longitudinal fasciculus, and inferior fronto-occipital fasciculus (see Figure 1c). Then, the mean signals in the orientational distortion were computed in these tracts of interest. Between-group comparisons were made between individuals with aMCI and CN, and multiple comparisons were corrected using the FDR correction with an alpha of .05. In addition, Pearson's correlation analysis was performed between cognitive scores and the tracts of interest that passed multiple comparisons corrections.

3.3 | The relationship between morphological measures and the orientational changes in the white matter fibers

Native space T1-weighted images were used to measure the total intracranial and lateral ventricular volume, total cerebral white matter volume and total gray matter volume using FreeSurfer 6.0 (See the Supporting Information). In order to explore the association of the

orientational changes of the white matter fibers with the morphological volume including: lateral ventricular, white matter volume and gray matter volume, Pearson's correlation was firstly used to examine whether the total distortion in the orientation of changed white matter was associated with these morphological volumes, respectively. When the relationships between total distortion and morphological volumes are significant, the corresponding morphological measures will be included as independent variables into the multiple linear regression models to investigate how these morphological metrics contribute to the changes in the orientation of white matter fibers. Finally, a voxel-wised generalized linear model was performed to investigate the association between total distortion and the most significant independent predictive factor in the above regression model. Age, sex, and scanner sites were included as nuisance covariates in the model. TFCE (Smith & Nichols, 2009) was used to correct for multiple comparisons across the whole brain at $p < .05$.

4 | RESULTS

4.1 | Clinical and demographic characteristics

Clinical and demographic characteristics of each diagnostic group are summarized in Table 1. There was no significant difference in either age or sex.

4.2 | Tract-based spatial statistics

As shown in Figure 2, AD patients had large-extent abnormalities in the orientation and integrity of white matter fibers in comparison with CN. Specifically, there was a significant increase of splay in the left corticospinal tract, and significant decrease of splay in the bilateral inferior longitudinal fasciculus and left uncinate fasciculus. Bend was found to be significantly greater in the bilateral corticospinal tract and forceps major, and less in the bilateral anterior thalamic radiation, inferior fronto-occipital fasciculus, inferior and superior longitudinal fasciculus, uncinate fasciculus, and left corticospinal tract. The significant twist increases in AD were mainly observed in the bilateral corticospinal tract, while the significant twist decreases were found in the bilateral anterior thalamic radiation, inferior fronto-occipital fasciculus, inferior and superior longitudinal fasciculus, uncinate fasciculus, and forceps minor. However, when aMCI patients were compared to CN individuals, we found no significant changes in the orientation or integrity of white matter fibers.

As shown in Figure 3, the green region showed where AD had significantly different bend index but not FA in comparison with CN. We visualized the tensor fields by coloring the glyphs using the bend index and FA in one of the significantly different regions (highlighted with a yellow box) in AD, aMCI, and CN. We can visually observe distinct geometric microstructural changes in the given region (yellow boxes), where bend index (lower box) had a significant increase while FA (upper box) is visually similar in AD, aMCI, and CN.
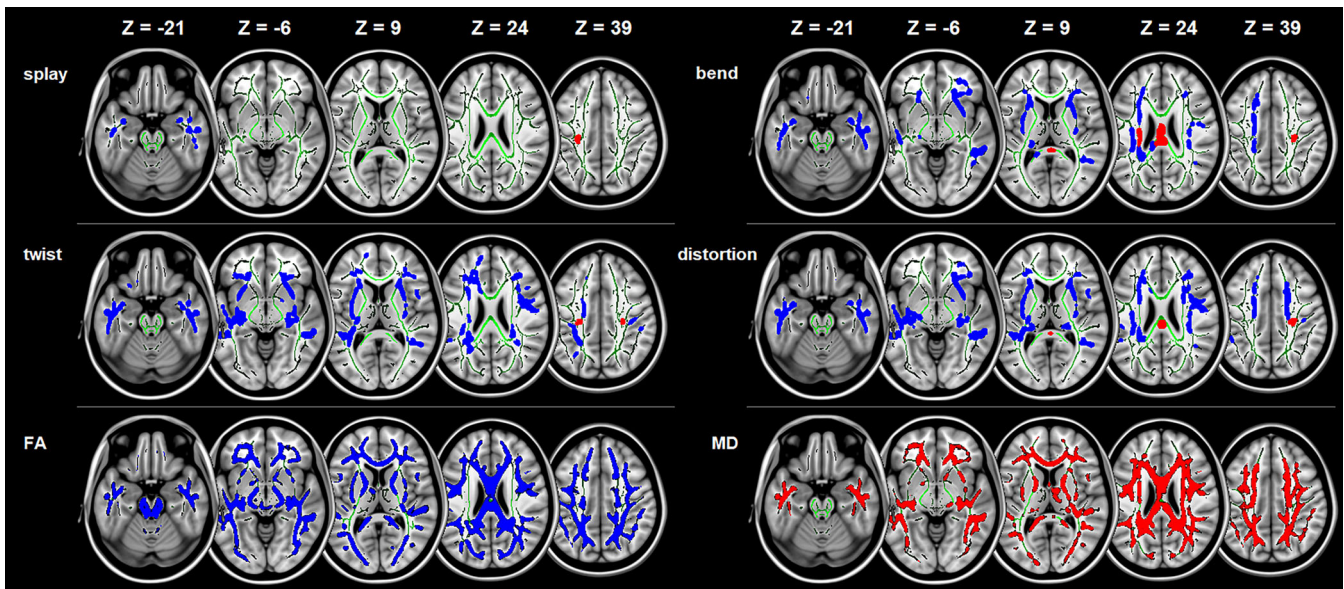
FIGURE 2 Micro-structural changes in the orientation and integrity in AD compared to CN across the whole brain white matter. Tract-Based Spatial Statistics white matter analysis showing a pattern of orientational changes (i.e., splay, bend, twist, and total distortion) and classical metrics (i.e., FA and MD) overlaid on the white matter skeleton (green) in individuals with Alzheimer's disease compared to cognitive normal individuals ($p < .05$, corrected for multiple comparisons). Blue is for the decrease, and Red is for the increase. AD, Alzheimer's disease; CN, cognitively normal; FA, fractional anisotropy; MD, mean diffusivity
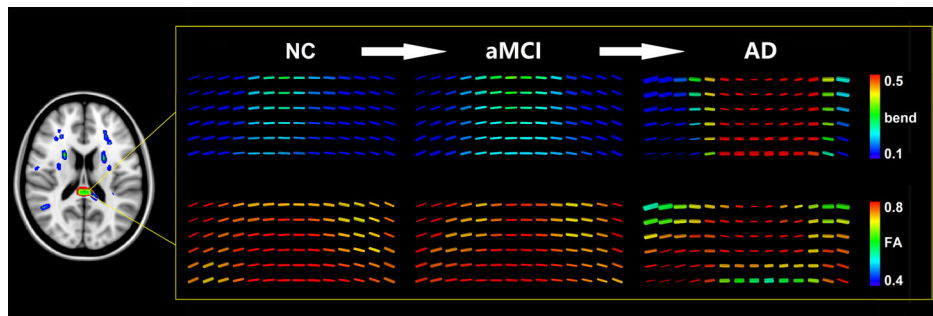

FIGURE 3 Sketch map of the significant increase of the bend index in the tensor field in AD compared to CN. The green region showed AD is significantly different with CN in bend but not FA. We visualized the tensor field by coloring the glyphs using the bend index and FA in one of the significant different regions (yellow boxes) in AD, MCI, and CN. We can visually observe the significant increase of the bend index in the tensor field (lower box) in the given region where the FA (upper box) is visually similar in AD, MCI, and CN. AD, Alzheimer's disease; CN, cognitively normal; FA, fractional anisotropy; MCI, mild cognitive impairment

4.3 | Tracts of interest analysis

As shown in Figure 4a. Compared to CN individuals, aMCI patients had significantly less splay in the left inferior longitudinal fasciculus (ILF; $t_{[114]} = -2.954$, corrected $p < .05$), and uncinate fasciculus (UF; $t_{[114]} = -2.425$, corrected $p < .05$). No other DFA metrics or FA, MD in any tracts of interest showed significant difference after the multiple comparison correction in aMCI compared to CN.

Meanwhile, we found a significant correlation between the cognitive scores and the splay in the orientation of white matter fiber within the left ILF (MMSE: $r = .289$, $p < .001$; MoCA: $r = .237$, $p = .003$. see Figure 4b). However, the cognitive scores had only a

trend of correlation with the splay within the left UF (MMSE: $r = .139$, $p = .077$; MoCA: $r = .141$, $p = .079$. see Figure 4b).

4.4 | The relationship between morphological measures and the orientational changes in the white matter fibers

As shown in Figure 5a–c, we found that the total distortion was significantly correlated with lateral ventricle volumes ($r = -.613$, $p < .001$), total cerebral white matter volume ($r = .215$, $p = .008$) and total gray matter volume ($r = .459$, $p < .001$).
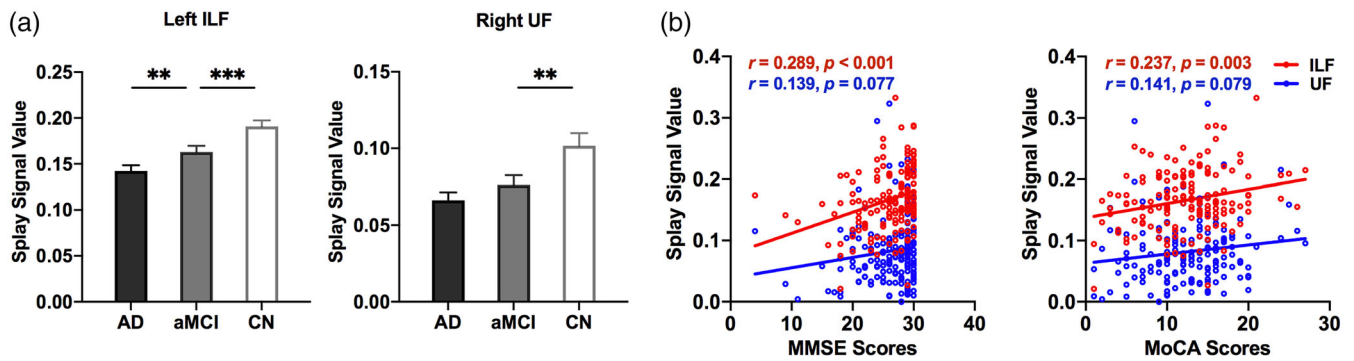
FIGURE 4 Tracts of interest analysis. (a) Comparison between CN, MCI, and AD. (b) Correlation between the splay of the orientation in tracts of interest and the cognitive performance. **, corrected $p < .05$; ***, corrected $p < .01$. AD, Alzheimer's disease; CN, cognitively normal; FA, fractional anisotropy; ILF, inferior longitudinal fasciculus; MCI, mild cognitive impairment; MoCA, Montreal cognitive assessment; MMSE, Mini-Mental State Exam; UF, uncinate fasciculus
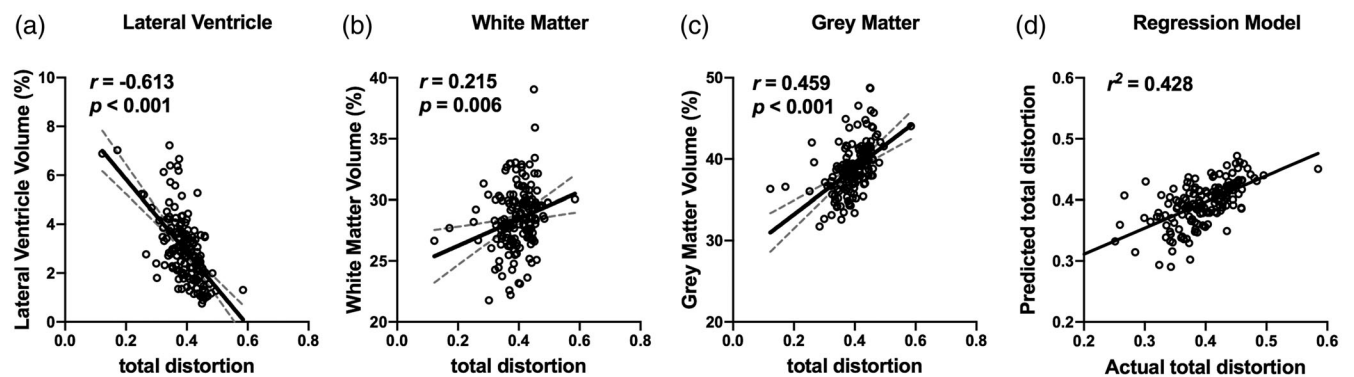

FIGURE 5 Association between morphological changes and orientational distortion. The total distortion was close association with lateral ventricular volume (a), total cerebral white matter volume (b), and total gray matter volume (c). Multiple linear regression models that contained of lateral ventricle volume, total cerebral white matter volume and total gray matter volume explained 42.8% of the variance of total distortion (d)

The multiple linear regression model revealed that the total distortion was independently associated with lateral ventricle volumes (standardized $\beta = -.524$, $p < .001$), total cerebral white matter volume (standardized $\beta = -.147$, $p = .049$), and total gray matter volume (standardized $\beta = .302$, $p < .001$) (Table 2). This model that contained of lateral ventricle volume, total cerebral white matter volume and total gray matter volume explained 42.8% of the variance of total distortion (Figure 5d).

As shown in Figure 6, in CN individuals, the lateral ventricular volume was significantly correlated with total distortion in the orientation of the white matter fibers. The correlated areas were mainly in the vicinity of the lateral ventricles including the genu, body, and splenium of corpus callosum. This is consistent with our hypothesis that the expansion of lateral ventricle has an impact on the orientation of white matter fibers in the surrounding areas. Interestingly, in patients with MCI or AD, we observed a negative correlation between the lateral ventricular volume and total distortion in the orientation within the junction of white matter and the cortex, which demonstrates that the disease progression may have a significant role in the orientational changes of local white matter region.

TABLE 2 The association of relevant morphological changes with total distortion in the changed white matter using multiple linear regression model

Model	β	Standardized β	t	p	R^2
Intercept	.350		7.047	<.001	.428
Lateral ventricular volume	−.022	−.524	−7.708	<.001	
White matter volume	−.003	−.147	−1.982	.049	
Gray matter volume	.005	.302	3.839	<.001	

Note: R^2 represents the proportion of variation in total distortion explained by all morphological variables in the multiple linear regression model.

5 | DISCUSSION

Our study is the first to examine the orientational changes of local white matter fibers in AD and aMCI. There are three primary findings in this study: (a) patients with AD exhibit spatially extensive
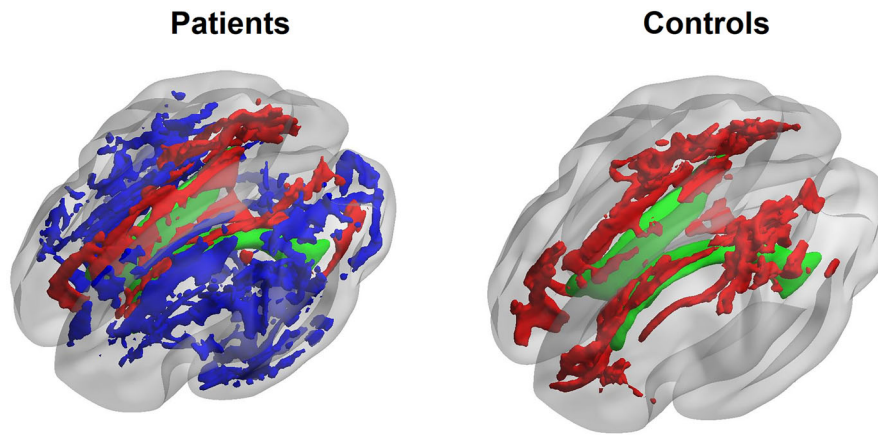
Patients   **Controls**

FIGURE 6 Voxel-wise association between the lateral ventricle volume and the orientational properties in white matter fibers. We can visually observe that areas showing significant positive correlation (depicted in green) mainly in the vicinity of the lateral ventricles (depicted in red) both in the cognitively normal individuals, and patients with AD and aMCI, confirming the morphological impact on the orientation of white matter fiber. Conversely, the negative correlated white matter areas (depicted in blue) were only observed in patients with AD and aMCI, and distributed in the junction of white matter and the cortex, suggesting an essential role of the disease progression in the orientational changes of white matter fibers. AD, Alzheimer's disease; aMCI, amnestic mild cognitive impairment

changes in the orientation of white matter fibers. These orientational changes of white matter fibers were mainly found in the bilateral anterior thalamic radiation, corticospinal tract, inferior and superior longitudinal fasciculus, inferior fronto-occipital fasciculus and uncinate fasciculus; (b) aMCI patients had subtle orientational changes in white matter fibers in the left inferior longitudinal fasciculus and right uncinate fasciculus, which showed a significant association with the cognitive performance. (c) The orientational change of white matter fibers observed in patients and cognitively normal individuals has a close association with lateral ventricular volume, total cerebral white matter volume and total gray matter volume, suggesting that the geometric microstructural changes in the orientation of white matter fibers were likely partially due to the morphological changes as the AD progress.

5.1 | Spatially extensive orientational changes of white matter fibers in AD

This study used a novel methodology to detect the orientational changes of local white matter fibers at an inter-voxel level in AD. We demonstrated that AD patients exhibit spatially extensive geometric microstructural changes in the orientation of white matter fibers around the whole brain. This was observed in the bilateral anterior thalamic radiation, corticospinal tract, inferior fronto-occipital fasciculus, inferior and superior longitudinal fasciculus, and uncinate fasciculus. This is consistent with previous reports on the pattern of microstructural white matter damages in AD (Benitez et al., 2014; Douaud et al., 2011; Mayo, Mazerolle, Ritchie, Fisk, & Gawryluk, 2017). For example, Mayo et al. (2017) demonstrated a similar widespread pattern of reduced FA and increased MD across the whole brain including the corticospinal tract, uncinate fasciculus, longitudinal fasciculus, and fronto-occipital fasciculus in AD compared to healthy controls. Furthermore, the sample

with high-risk AD also showed a similar decreased microstructural integrity in specific white matter tracts, suggesting that these disruptions represent a very remarkable feature in the course of AD (Gold, Powell, Andersen, & Smith, 2010).

Of note, we observed the increase in all three geometric microstructural properties of the orientation in the white matter fibers surrounding the lateral ventricles, mainly in the corpus callosum and part of corticospinal tract. It may be a consequence of ventricular dilatation to distort the orientation of peri-ventricle white matter fibers (Chou et al., 2009). This is in line with our observed positive association between lateral ventricle and the orientational distortion in corpus callosum both in CN individuals and in patients with AD and aMCI. Furthermore, we found the decrease in the orientation of the late-myelinating white matter tracts including fronto-occipital fasciculus, longitudinal fasciculus and uncinate fasciculus. Late-myelinating regions in brain development contain smaller axons with fewer myelin lamellae (Chia, Thompson, & Moscarello, 1983). These regions thus tend to be more vulnerable to breakdown by neurodegenerative brain disorders such as AD (Kemper, 1994). The preferential vulnerability of late-myelinating areas in AD first develop in areas that are last to myelinate prior to affecting early-myelinating areas (Braak & Braak, 1996), and that a loss of myelin accounts for cognitive decline (Peters et al., 1996). In accord to other studies (Brickman et al., 2012; Stricker et al., 2009), our study contributes to clarify the particular tissue properties of late-myelinating white matter fibers that underwent aberrant changes both in the orientation and integrity of microstructure through the course of AD.

5.2 | Subtle orientational changes of white matter fibers in aMCI

The preferential vulnerability of late-myelinating areas to aging and AD is a proposed mechanism by which cognition declines, referred to

as "retrogenesis" (Benitez et al., 2014; Reisberg et al., 1999). Amnestic mild cognitive impairment represents a transitional state between normal aging and early dementia. Consequently, the degeneration of late-myelinating white matter fibers may have appeared in the prodromal phase of AD (i.e., aMCI; Shao et al., 2019). In agreement with this view, our results pointed to the subtle geometric microstructural degeneration of the orientation in the left inferior longitudinal fasciculus and right uncinate fasciculus in aMCI, and the association of these orientational distortions with cognitive impairment. The findings suggest that the breakdown of these late-myelinating areas may promote the development of aMCI, which could become a specific neuroimaging marker to distinguish between aMCI and CN (Makovac et al., 2018; Zhuang et al., 2013).

Structural connections are deemed to be the essential foundation for the information flow of interneural communication across different cerebral regions, and underlie the normal cognitive function (Liu et al., 2017; Mito et al., 2018; Teipel et al., 2010). The inferior longitudinal fasciculus and uncinate fasciculus constitutes the long-range association fibers of the anterior temporal lobes with the occipital cortex, and orbitofrontal and dorsolateral prefrontal cortex, respectively (Latini et al., 2017; Von Der Heide, Skipper, Klobusicky, & Olson, 2013). Portions of the anterior temporal lobe are believed to play an essential role in certain types of semantic memory (Patterson, Nestor, & Rogers, 2007), and also in the encoding and storage of social and emotional concepts (Olson, McCoy, Klobusicky, & Ross, 2013). In addition, previous evidences have highlighted the involvement of inferior longitudinal fasciculus and uncinate fasciculus in episodic and semantic memory, language, and social emotional processing (Hodgetts et al., 2017; Mandonnet, Nouet, Gatignol, Capelle, & Duffau, 2007; Von Der Heide et al., 2013). As such, the degeneration of the inferior longitudinal fasciculus and uncinate fasciculus in aMCI would logically affect the normally bidirectional information transmission of orbital frontal cortex-based feedback and visual cues to rapidly modulate temporal lobe-based mnemonic representations (Von Der Heide et al., 2013). Therefore, the observed disruptions of inferior longitudinal fasciculus and uncinate fasciculus in our study may reflect the functional disconnection within the networks subserving the memory and language, and to some extent contribute to the gradual onset of cognitive dysfunction in aMCI (Dziemian, Appenzeller, von Bastian, Jäncke, & Langer, 2021; Metzler-Baddeley, Jones, Belaroussi, Aggleton, & Sullivan, 2011).

5.3 | The underlying contributors to orientational changes of white matter fibers in AD

Compared to classical intravoxel metrics (e.g., FA and MD) which to some extent reflect the integrity of microstructure in the white matter fibers, the intervoxel-based DFA metrics focus on the orientational properties of microstructure in the white matter fibers, that is, it considers in some sense a kind of local atrophy or swelling in the microstructure of the white matter fibers (see Figure 3). We postulate that this geometric microstructure in the orientation of white matter fibers may be partially caused by morphological changes (i.e., dilation of ventricles, white matter atrophy, and gray matter atrophy) during aging and disease progression. This hypothesis is confirmed by our results of correlation analysis, which are line with previous findings that aging processes and disease progression are associated with apparent ventricular dilation, white matter atrophy and gray matter atrophy (Balthazar et al., 2009; Biegon et al., 1994; Bramlett & Dietrich, 2002; Chou et al., 2009; Ferreira et al., 2011; Guo et al., 2010; Tabatabaei-Jafari et al., 2015; Thompson et al., 2004). Aside from this, ventricular dilation made the most contribution to geometric microstructural changes in the orientation of white matter fibers, especially in the vicinity of the lateral ventricles, such as the corpus callosum. Interestingly, negative correlation was observed in the junction of white matter and the cortex in patients with AD and aMCI, which may suggest an essential role of disease progression in the orientational changes of white matter fibers. In other words, neural loss and glial swelling during the AD progression may lead to changes in the orientation of white matter fibers (Shu et al., 2013; Zerbi et al., 2013). Axonal loss and glial swelling are prominent features of AD (Englund, 1998; Stokin et al., 2005), this may lead to the enlarged perivascular spaces in the pathogenesis of AD (Fischer & Maier, 2015; Kawahara, 2010; Leszek et al., 2016; Reddy, 2009; Santos et al., 2010; Shu et al., 2013). Therefore, neural loss, glial swelling itself, and its subsequent impact on enlarged perivascular spaces may also be another possible explanation for the geometric microstructural changes in the orientation of white matter fibers in AD.

5.4 | Limitation and future direction

The present study has several limitations. One limitation is that the voxel-based DFA method used in this manuscript considers the principal directions in voxels estimated by DTI, thus, it is not sensitive enough to those voxels with crossing directions. It could be a future work to calculate DFA indices based on fiber directions estimated by spherical deconvolution methods (Cheng, Deriche, Jiang, Shen, & Yap, 2014; Tournier, Calamante, Gadian, & Connelly, 2004), and perform fixel-based analysis (Raffelt et al., 2012). We also plan to perform tract-based DFA (Cheng et al., 2018) to calculate the orientational properties from fiber tracts estimated after tractography, and perform fiber-base analysis (Raffelt et al., 2012). Another major question was that we used a cross-sectional study design, which prevented us from determining which aMCI converted to AD. Future studies should investigate longitudinally the progression of aMCI and AD to see whether the orientational changes of white matter fibers in aMCI is indeed an early feature of AD or other pathologies. Finally, the finding about the inferior longitudinal fasciculus and uncinate fasciculus in aMCI needs to further be examined to understand its implications for predicting progression of aMCI to AD. Unlike AD, aMCI is rather heterogeneous in its underlying pathology. Many pathologies could underlie aMCI, such as white matter lesions, stroke, and cerebral atrophy (Jicha et al., 2006; Larrieu, Letenneur, Orgogozo, Fabrigoule, & Amieva, 2002). Futures studies should pay more attention to verifying the potential biomarker of inferior longitudinal fasciculus and uncinate fasciculus in more aging-related pathologies.

6 | CONCLUSION

This study investigated aMCI and AD patients using the newly established geometric microstructural measures in the orientation of white matter fibers. The study showed that AD patients had a specific pattern of orientational changes throughout white matter regions. On the other hand, aMCI patients showed subtle geometric microstructural changes of the orientation in the left inferior longitudinal fasciculus and right uncinate fasciculus, which underpinned the cognitive impairment. Intrinsically, these observed orientational changes in AD may be a consequence of morphological alterations and neuropathological damage. Together, our findings demonstrated that the orientational information of white matter fibers could provide novel insights into the underlying biological and pathological mechanism of AD and aMCI.

CONFLICT OF INTERESTS

The authors declare no potential conflict of interest.

DATA AVAILABILITY STATEMENT

The dataset used and analyzed are available to other researchers' subject to review of the request by the Scientific Committee of the study and ethics approval. All imaging, demographics, and neuropsychological data used in this article are publicly available and were downloaded from the ADNI website (adni.loni.usc.edu). Upon request, we will provide a list of ADNI participant identifications for replication purposes.

ETHICS STATEMENT

Ethics approval was obtained by the ADNI investigators. Written informed consent was obtained from all individuals participating in the study according to the Declaration of Helsinki.

ORCID

Tao Liu https://orcid.org/0000-0002-7783-3073
Perminder S. Sachdev https://orcid.org/0000-0002-9595-3220

REFERENCES

Apostolova, L. G., Mosconi, L., Thompson, P. M., Green, A. E., Hwang, K. S., Ramirez, A., … de Leon, M. J. (2010). Subregional hippocampal atrophy predicts Alzheimer's dementia in the cognitively normal. *Neurobiology of Aging, 31*, 1077–1088.

Apostolova, L. G., & Thompson, P. M. (2008). Mapping progressive brain structural changes in early Alzheimer's disease and mild cognitive impairment. *Neuropsychologia, 46*, 1597–1612.

Balthazar, M. L. F., Yasuda, C. L., Pereira, F. R., Pedro, T., Damasceno, B. P., & Cendes, F. (2009). Differences in grey and white matter atrophy in amnestic mild cognitive impairment and mild Alzheimer's disease. *European Journal of Neurology, 16*, 468–474.

Bartzokis, G. (2011). Alzheimer's disease as homeostatic responses to age-related myelin breakdown. *Neurobiology of Aging, 32*, 1341–1371.

Benitez, A., Fieremans, E., Jensen, J. H., Falangola, M. F., Tabesh, A., Ferris, S. H., & Helpern, J. A. (2014). White matter tract integrity metrics reflect the vulnerability of late-myelinating tracts in Alzheimer's disease. *NeuroImage: Clinical, 4*, 64–71.

Biegon, A., Eberling, J., Richardson, B., Roos, M., Wong, S., Reed, B. R., & Jagust, W. (1994). Human corpus callosum in aging and Alzheimer's disease: A magnetic resonance imaging study. *Neurobiology of Aging, 15*, 393–397.

Braak, H., & Braak, E. (1991). Demonstration of amyloid deposits and neurofibrillary changes in whole brain sections. *Brain Pathology, 1*, 213–216.

Braak, H., & Braak, E. (1995). Staging of alzheimer's disease-related neurofibrillary changes. *Neurobiology of Aging, 16*, 271–278.

Braak, H., & Braak, E. (1996). Development of Alzheimer-related neurofibrillary changes in the neocortex inversely recapitulates cortical myelogenesis. *Acta Neuropathologica, 92*, 197–201.

Bramlett, H. M., & Dietrich, D. W. (2002). Quantitative structural changes in white and gray matter 1 year following traumatic brain injury in rats. *Acta Neuropathologica, 103*, 607–614.

Brickman, A. M., Meier, I. B., Korgaonkar, M. S., Provenzano, F. A., Grieve, S. M., Siedlecki, K. L., … Zimmerman, M. E. (2012). Testing the white matter retrogenesis hypothesis of cognitive aging. *Neurobiology of Aging, 33*, 1699–1715.

Canter, R. G., Penney, J., & Tsai, L. H. (2016). The road to restoring neural circuits for the treatment of Alzheimer's disease. *Nature, 539*, 187–196.

Cheng, J., & Basser, P. J. (2017). Director field analysis (DFA): Exploring local white matter geometric structure in diffusion MRI. *Medical Image Analysis, 43*, 112–128.

Cheng, J., Deriche, R., Jiang, T., Shen, D., & Yap, P.-T. (2014). Non-negative spherical deconvolution (NNSD) for estimation of fiber orientation distribution function in single−/multi-shell diffusion MRI. *NeuroImage, 101*, 750–764.

Cheng, J., Liu, T., Shi, F., Bai, R., Zhang, J., Zhu, H., … Basser, P. J. (2018). On quantifying local geometric structures of fiber tracts. In A. F. Frangi, J. A. Schnabel, C. Davatzikos, C. Alberola-López,

G. Fichtinger (eds.). *Medical Image Computing and Computer Assisted Intervention – MICCAI 2018*. (Vol. 11072, pp. 392–400). Lecture Notes in Computer Science. Cham, Switzerland: Springer.

Chia, L. S., Thompson, J. E., & Moscarello, M. A. (1983). Changes in lipid phase behaviour in human myelin during maturation and aging. *FEBS Letters*, 157, 155–158.

Chintamaneni, M., & Bhaskar, M. (2012). Biomarkers in Alzheimer's disease: A review. *ISRN Pharmacology*, 2012, 1–6.

Chou, Y.-Y., Leporé, N., Avedissian, C., Madsen, S. K., Parikshak, N., Hua, X., … Toga, A. W. (2009). Mapping correlations between ventricular expansion and CSF amyloid and tau biomarkers in 240 subjects with Alzheimer's disease, mild cognitive impairment and elderly controls. *NeuroImage*, 46, 394–410.

Desikan, R. S., Sabuncu, M. R., Schmansky, N. J., Reuter, M., Cabral, H. J., Hess, C. P., … Initiative, t.A.s.D.N. (2010). Selective disruption of the cerebral Neocortex in Alzheimer's disease. *PLoS One*, 5, e12853.

Douaud, G., Jbabdi, S., Behrens, T. E. J. J., Menke, R. A., Gass, A., Monsch, A. U., … Smith, S. (2011). DTI measures in crossing-fibre areas: Increased diffusion anisotropy reveals early white matter alteration in MCI and mild Alzheimer's disease. *NeuroImage*, 55, 880–890.

Dziemian, S., Appenzeller, S., von Bastian, C. C., Jäncke, L., & Langer, N. (2021). Working memory training effects on white matter integrity in young and older adults. *Frontiers in Human Neuroscience*, 15, 605213–605213.

Englund, E. (1998). Neuropathology of white matter changes in Alzheimer's disease and vascular dementia. *Dementia and Geriatric Cognitive Disorders*, 9, 6–12.

Ferreira, L. K., Diniz, B. S., Forlenza, O. V., Busatto, G. F., & Zanetti, M. V. (2011). Neurostructural predictors of Alzheimer's disease: A meta-analysis of VBM studies. *Neurobiology of Aging*, 32, 1733–1741.

Fischer, R., & Maier, O. (2015). Interrelation of oxidative stress and inflammation in neurodegenerative disease: Role of TNF. *Oxidative Medicine and Cellular Longevity*, 2015, 1–18.

Gold, B. T., Johnson, N. F., Powell, D. K., & Smith, C. D. (2012). White matter integrity and vulnerability to Alzheimer's disease: Preliminary findings and future directions. *Biochimica et Biophysica Acta (BBA)— Molecular Basis of Disease*, 1822, 416–422.

Gold, B. T., Powell, D. K., Andersen, A. H., & Smith, C. D. (2010). Alterations in multiple measures of white matter integrity in normal women at high risk for Alzheimer's disease. *NeuroImage*, 52, 1487–1494.

Guo, X., Wang, Z., Li, K., Li, Z., Qi, Z., Jin, Z., … Chen, K. (2010). Voxel-based assessment of gray and white matter volumes in Alzheimer's disease. *Neuroscience Letters*, 468, 146–150.

Hodgetts, C. J., Postans, M., Warne, N., Varnava, A., Lawrence, A. D., & Graham, K. S. (2017). Distinct contributions of the fornix and inferior longitudinal fasciculus to episodic and semantic autobiographical memory. *Cortex*, 94, 1–14.

Hua, X., Hibar, D. P., Ching, C. R. K., Boyle, C. P., Rajagopalan, P., Gutman, B. A., … Thompson, P. M. (2013). Unbiased tensor-based morphometry: Improved robustness and sample size estimates for Alzheimer's disease clinical trials. *NeuroImage*, 66, 648–661.

Jicha, G. A., Parisi, J. E., Dickson, D. W., Johnson, K., Cha, R., Ivnik, R. J., … Petersen, R. C. (2006). Neuropathologic outcome of mild cognitive impairment following progression to clinical dementia. *Archives of Neurology*, 63, 674–681.

Jones, D. K., Knösche, T. R., & Turner, R. (2013). White matter integrity, fiber count, and other fallacies: The do's and don'ts of diffusion MRI. *NeuroImage*, 73, 239–254.

Kawahara, M. (2010). Neurotoxicity of β-amyloid protein: Oligomerization, channel formation and calcium dyshomeostasis. *Current Pharmaceutical Design*, 16, 2779–2789.

Kemper, T. L. (1994). *Neuroanatomical and neuropathological changes during aging and dementia. Clinical neurology of aging* (2nd ed., pp. 3–67). New York, NY: Oxford University Press.

Langen, C. D., Zonneveld, H. I., White, T., Huizinga, W., Cremers, L. G. M., de Groot, M., … Vernooij, M. W. (2017). White matter lesions relate to tract-specific reductions in functional connectivity. *Neurobiology of Aging*, 51, 97–103.

Larrieu, S., Letenneur, L., Orgogozo, J. M., Fabrigoule, C., & Amieva, H. (2002). Incidence and outcome of mild cognitive impairment in a population-based. *American Academy of Neurology*, 59, 1594–1599.

Latini, F., Mårtensson, J., Larsson, E.-M., Fredrikson, M., Åhs, F., Hjortberg, M., … Ryttlefors, M. (2017). Segmentation of the inferior longitudinal fasciculus in the human brain: A white matter dissection and diffusion tensor tractography study. *Brain Research*, 1675, 102–115.

Leszek, J., Barreto, E., Gasiorowski, K., Koutsouraki, E., & Aliev, G. (2016). Inflammatory mechanisms and oxidative stress as key factors responsible for progression of neurodegeneration: role of brain innate immune system. *CNS & Neurological Disorders-Drug Targets (Formerly Current Drug Targets-CNS & Neurological Disorders)*, 15, 329–336.

Leung, K. K., Bartlett, J. W., Barnes, J., Manning, E. N., Ourselin, S., & Fox, N. C. (2013). Cerebral atrophy in mild cognitive impairment and Alzheimer disease: Rates and acceleration. *Neurology*, 80, 648–654.

Leung, L. H., Ooi, G.-C., Kwong, D. L., Chan, G. C., Cao, G., & Khong, P.-L. (2004). White-matter diffusion anisotropy after chemo-irradiation: A statistical parametric mapping study and histogram analysis. *NeuroImage*, 21, 261–268.

Liu, H., Yang, Y., Xia, Y., Zhu, W., Leak, R. K., Wei, Z., … Hu, X. (2017). Aging of cerebral white matter. *Ageing Research Reviews*, 34, 64–76.

Makovac, E., Serra, L., Di Domenico, C., Marra, C., Caltagirone, C., Cercignani, M., & Bozzali, M. (2018). Quantitative magnetization transfer of white matter tracts correlates with diffusion tensor imaging indices in predicting the conversion from mild cognitive impairment to Alzheimer's disease. *Journal of Alzheimer's Disease*, 63, 561–575.

Mandonnet, E., Nouet, A., Gatignol, P., Capelle, L., & Duffau, H. (2007). Does the left inferior longitudinal fasciculus play a role in language? A brain stimulation study. *Brain*, 130, 623–629.

Mayo, C. D., Mazerolle, E. L., Ritchie, L., Fisk, J. D., & Gawryluk, J. R. (2017). Longitudinal changes in microstructural white matter metrics in Alzheimer's disease. *NeuroImage: Clinical*, 13, 330–338.

Metzler-Baddeley, C., Jones, D. K., Belaroussi, B., Aggleton, J. P., & Sullivan, M. J. (2011). Frontotemporal connections in episodic memory and aging: A diffusion MRI tractography study. *The Journal of Neuroscience*, 31, 13236–13245.

Minati, L., Edginton, T., Grazia Bruzzone, M., & Giaccone, G. (2009). Reviews: Current concepts in Alzheimer's disease: A multidisciplinary review. *American Journal of Alzheimer's Disease & Other Dementias*, 24, 95–121.

Mito, R., Raffelt, D., Dhollander, T., Vaughan, D. N., Tournier, J. D., Salvado, O., … Connelly, A. (2018). Fibre-specific white matter reductions in Alzheimer's disease and mild cognitive impairment. *Brain*, 141, 888–902.

Mori, S., Oishi, K., Jiang, H., Jiang, L., Li, X., Akhter, K., … Mazziotta, J. (2008). Stereotaxic white matter atlas based on diffusion tensor imaging in an ICBM template. *NeuroImage*, 40, 570–582.

Nachev, P., Wydell, H., O'neill, K., Husain, M., & Kennard, C. (2007). The role of the pre-supplementary motor area in the control of action. *Neuroimage*, 36, T155–T163.

Nir, T. M., Jahanshad, N., Villalon-Reina, J. E., Toga, A. W., Jack, C. R., Weiner, M. W., … Initiative, A.s.D.N. (2013). Effectiveness of regional DTI measures in distinguishing Alzheimer's disease, MCI, and normal aging. *NeuroImage: Clinical*, 3, 180–195.

O'Donnell, L. J., & Pasternak, O. (2015). Does diffusion MRI tell us anything about the white matter? An overview of methods and pitfalls. *Schizophrenia Research*, 161, 133–141.

Olson, I. R., McCoy, D., Klobusicky, E., & Ross, L. A. (2013). Social cognition and the anterior temporal lobes: A review and theoretical framework. *Social Cognitive and Affective Neuroscience*, 8, 123–133.

Palop, J. J., Chin, J., & Mucke, L. (2006). A network dysfunction perspective on neurodegenerative diseases. *Nature*, *443*, 768–773.

Patterson, K., Nestor, P. J., & Rogers, T. T. (2007). Where do you know what you know? The representation of semantic knowledge in the human brain. *Nature Reviews Neuroscience*, *8*, 976–987.

Peters, A., Rosene, D. L., Moss, M. B., Kemper, T. L., Abraham, C. R., Tigges, J., & Albert, M. S. (1996). Neurobiological bases of age-related cognitive decline in the rhesus monkey. *Journal of Neuropathology and Experimental Neurology*, *55*, 861–874.

Qin, Y.-Y., Li, M.-W., Zhang, S., Zhang, Y., Zhao, L.-Y., Lei, H., ... Zhu, W.-Z. (2013). In vivo quantitative whole-brain diffusion tensor imaging analysis of APP/PS1 transgenic mice using voxel-based and atlas-based methods. *Neuroradiology*, *55*, 1027–1038.

Raffelt, D., Tournier, J. D., Rose, S., Ridgway, G. R., Henderson, R., Crozier, S., ... Connelly, A. (2012). Apparent fibre density: A novel measure for the analysis of diffusion-weighted magnetic resonance images. *NeuroImage*, *59*, 3976–3994.

Reddy, P. H. (2009). Amyloid beta, mitochondrial structural and functional dynamics in Alzheimer's disease. *Experimental Neurology*, *218*, 286–292.

Reisberg, B., Franssen, E. H., Hasan, S. M., Monteiro, I., Boksay, I., Souren, L. E. M., ... Kluger, A. (1999). Retrogenesis: Clinical, physiologic, and pathologic mechanisms in brain aging, Alzheimer's and other dementing processes. *European Archives of Psychiatry and Clinical Neuroscience*, *249*, S28–S36.

Santos, R. X., Correia, S. C., Wang, X., Perry, G., Smith, M. A., Moreira, P. I., & Zhu, X. (2010). Alzheimer's disease: Diverse aspects of mitochondrial malfunctioning. *International Journal of Clinical and Experimental Pathology*, *3*, 570.

Shao, W., Li, X., Zhang, J., Yang, C., Tao, W., Zhang, S., ... Peng, D. (2019). White matter integrity disruption in the pre-dementia stages of Alzheimer's disease: From subjective memory impairment to amnestic mild cognitive impairment. *European Journal of Neurology*, *26*, 800–807.

Shu, X., Qin, Y.-Y., Zhang, S., Jiang, J.-J., Zhang, Y., Zhao, L.-Y., ... Zhu, W.-Z. (2013). Voxel-based diffusion tensor imaging of an APP/PS1 mouse model of Alzheimer's disease. *Molecular Neurobiology*, *48*, 78–83.

Smith, S. M. (2002). Fast robust automated brain extraction. *Human Brain Mapping*, *17*, 143–155.

Smith, S. M., Jenkinson, M., Johansen-Berg, H., Rueckert, D., Nichols, T. E., Mackay, C. E., ... Behrens, T. E. J. (2006). Tract-based spatial statistics: Voxelwise analysis of multi-subject diffusion data. *NeuroImage*, *31*, 1487–1505.

Smith, S. M., & Nichols, T. E. (2009). Threshold-free cluster enhancement: Addressing problems of smoothing, threshold dependence and localisation in cluster inference. *NeuroImage*, *44*, 83–98.

Stokin, G. B., Lillo, C., Falzone, T. L., Brusch, R. G., Rockenstein, E., Mount, S. L., ... Williams, D. S. (2005). Axonopathy and transport deficits early in the pathogenesis of Alzheimer's disease. *Science*, *307*, 1282–1288.

Stricker, N. H., Schweinsburg, B. C., Delano-Wood, L., Wierenga, C. E., Bangen, K. J., Haaland, K. Y., ... Bondi, M. W. (2009). Decreased white matter integrity in late-myelinating fiber pathways in Alzheimer's disease supports retrogenesis. *NeuroImage*, *45*, 10–16.

Tabatabaei-Jafari, H., Shaw, M. E., & Cherbuin, N. (2015). Cerebral atrophy in mild cognitive impairment: A systematic review with meta-analysis. *Alzheimers & Dementia (Amsterdam, Netherlands)*, *1*, 487–504.

Taylor, W. D., Hsu, E., Krishnan, K. R. R., & MacFall, J. R. (2004). Diffusion tensor imaging: Background, potential, and utility in psychiatric research. *Biological Psychiatry*, *55*, 201–207.

Teipel, S. J., Bokde, A. L. W., Meindl, T., Amaro, E., Soldner, J., Reiser, M. F., ... Hampel, H. (2010). White matter microstructure underlying default mode network connectivity in the human brain. *NeuroImage*, *49*, 2021–2032.

Thompson, P. M., Hayashi, K. M., de Zubicaray, G. I., Janke, A. L., Rose, S. E., Semple, J., ... Doddrell, D. M. (2004). Mapping hippocampal and ventricular change in Alzheimer disease. *NeuroImage*, *22*, 1754–1766.

Tournier, J. D., Calamante, F., Gadian, D. G., & Connelly, A. (2004). Direct estimation of the fiber orientation density function from diffusion-weighted MRI data using spherical deconvolution. *NeuroImage*, *23*, 1176–1185.

Von Der Heide, R. J., Skipper, L. M., Klobusicky, E., & Olson, I. R. (2013). Dissecting the uncinate fasciculus: Disorders, controversies and a hypothesis. *Brain*, *136*, 1692–1707.

Wakana, S., Caprihan, A., Panzenboeck, M. M., Fallon, J. H., Perry, M., Gollub, R. L., ... Mori, S. (2007). Reproducibility of quantitative tractography methods applied to cerebral white matter. *NeuroImage*, *36*, 630–644.

Zerbi, V., Kleinnijenhuis, M., Fang, X., Jansen, D., Veltien, A., Van Asten, J., ... Heerschap, A. (2013). Gray and white matter degeneration revealed by diffusion in an Alzheimer mouse model. *Neurobiology of Aging*, *34*, 1440–1450.

Zhuang, L., Sachdev, P. S., Trollor, J. N., Reppermund, S., Kochan, N. A., Brodaty, H., & Wen, W. (2013). Microstructural white matter changes, not hippocampal atrophy, detect early amnestic mild cognitive impairment. *PLoS One*, *8*, e58887.

SUPPORTING INFORMATION

Additional supporting information may be found in the online version of the article at the publisher's website.